COBEM 2023 27TH INTERNATIONAL CONGRESS OF MECHANICAL ENGENEERING

ABCM Brazilian Society of Mechanical Sciences and Engineering
27th ABCM International Congress of Mechanical Engineering
December 04-08, 2023, Florianópolis-SC, Brazil

# COB-2023-1532 - STUDIES ABOUT THE DIMENSIONING OF FLANGED UNIONS OF INDUSTRIAL VALVES FOR APPLICATIONS IN OIL & GAS INSTALLATIONS

**Felipe Frizon**
**Diego Rizzotto Rossetto**
Federal Technological University of Paraná - Via do Conhecimento, s/n - KM 01- 85503-390 - Fraron, Pato Branco /PR Brazil
frizon@alunos.utfpr.edu.br, diegorossetto@utfpr.edu.br

**Diógenes Barbosa Teles**
Micromazza - BR-470, 168, Vila Flores - RS - 95334-000 - Brazil
dbteles.eng@gmail.com

***Abstract.*** *Among the various industrial sectors, the Oil & Gas industry is one of the main consumers of valves. These devices are used in the management of fluids in liquid, gas, or mixed states, playing a fundamental role in the production and safety of installations. Industrial valves are designed according to the requirements of international standards and technical specifications that require analytical structural calculations to provide adequate levels of reliability and safety for the installations, according to the pipeline pressure class. Among the parts of this equipment, the flange system of the body and its studied union have extreme importance in ensuring the ability to contain the fluid pressure internally within the equipment casing. In this context, the present study presents a calculation methodology based on the ASME code for sizing the flanged union of an onshore application ball valve. A case study will be addressed related to the sizing of the flanged union of the body of an industrial trunnion ball valve with a nominal passage diameter of 6", pressure class 600, and ASME 16.34 and API 6D construction standards. The analytical calculation methodology will be complemented by finite element method analyses, including linear elastic and elastic-plastic analysis, using ANSYS software following ASME VIII, Division II guidelines. The aim of this study is to propose a valve with constructive characteristics that meet the required safety criteria and to present a reference work for assistance in the sizing of this important equipment to the academic and industrial communities.*

***Keywords:*** *Industrial valves, Flanged unions, Analytical calculations, FEA*

## 1. INTRODUCTION

With the advent of agriculture, civilization had the need to manipulate the flow of rivers and streams for the irrigation process. Thus, ancient peoples such as the Egyptians and Mesopotamians created gate systems to control the water flow in channels. These systems evolved over time, with the development of bronze valves by the Greeks and Romans, up to the present day, where valves play a vital role in the control, stopping, and retention of fluids in industrial processes (SKOUSEN, 2011).

Among various industrial processes, the oil and gas sector, is one of the main consumers of valves. It is estimated that due to the importance of these components, valves account for 6% to 10% of the total cost of a petrochemical plant, reaching 20% to 30% of the cost related to piping (MORAES, 2005). Thus, this sector is one of the most demanding in terms of sophistication and innovation in valve design, with the development of technologies aiming at cost reduction and, above all, safety. This is because, given the complexity of the oil and gas sector, failures can have catastrophic consequences in terms of economic and socio-environmental aspects (ECOM, 2020).

The oil and gas industry extensively utilizes ball valves, as they transport powerful fluids and gases that require quick and secure shut-off. These valves offer reliable sealing when closed, low pressure loss, as well as precise and fast opening and closing. They belong to the quarter-turn valve family, which uses a hollow, perforated, and pivoting ball to block the flow (JEFFERSON, 2020).

In the design and manufacturing of ball valves used in the oil and gas industry, requirements are established through internationally recognized standards by manufacturers and customers of these components. Among the internationally applicable standards are API 6D (2014) and ASME B16-34 (2020); in Brazil, ABNT NBR 15827 (2018) is also accepted. These standards define coefficients, parameters, and calculation methods to size the geometry, materials, seals, testing, and operation of the valves. This method is known as 'design by rules' by ASME VIII Division II. Additionally, there is an alternative methodology called design by analysis, which allows for the application of numerical analysis using the finite element method.

The design by analysis methodology of ASME VIII Division II aims to protect against plastic collapse, using methods such as elastic stress, limit load, and elastic-plastic stress. It also considers localized failures through the elastic stress

method and the elastic-plastic deformation method. In addition, cyclic failures are assessed using the fatigue analysis method. However, it is important to note that the ASME VIII Division II standard was developed for the design of boilers and pressure vessels, not specifically for valves. Nevertheless, due to the lack of literature and technical standards specifying analysis procedures for valves, the main design standards make reference to the design by analysis method of ASME VIII Division II (ROSSETTO, 2016).

Following the concepts of standards-based design and analysis, this article aims to design a NPS6, Class 600, two-piece trunnion-mounted ball valve, using criteria defined by ASME B16.34, API 6D, and ABNT NBR 15827 (2018). Analytical calculation parameters will be evaluated to size the flanges, bolts, body, and cover of the valve. After sizing, a numerical model will be created using the finite element method with the assistance of the commercial software ANSYS. Through this model, analyses of elastic stresses will be performed, utilizing stress linearization, as well as analyses of elastic-plastic stresses and localized elastic-plastic deformations. The objective is to achieve a ball valve geometry that meets the requirements of structural collapse resistance and prevention of localized failures with an acceptable margin of safety.

## 2. CASE STUDY

### 2.1 Ball valve

According to Sotoodeh (2021), ball valves are widely used in operations involving aggressive media such as hydrocarbons, oil, and gas. These valves are designed to operate in the fully open or fully closed positions, with their main function not being flow control. This is due to their operational mechanism, which consists of a hollow, perforated, and pivoting ball housed within a tubular body. The flow of the fluid is controlled by the open bore of the ball: when the opening is fully aligned with the pipeline, the fluid passes through freely; in the closed position, the ball's bore is perpendicular to the direction of flow, blocking the passage. The rotational movement of the ball occurs within a range of 0º to 90º relative to the flow direction in the pipeline, allowing for the opening or closing of the valve.

Regarding the construction standards of ball valves, there are two types of ball-to-body sealing: floating ball and trunnion. In floating ball valves, the sealing is achieved through the movement of the ball, which causes deformation in the downstream seat. The sealing efficiency is directly influenced by the flow pressure on the upstream face. These valves are recommended for low-pressure lines due to the high operational torque and wear on the downstream seat. It is crucial to maintain an appropriate pressure to prevent leakage around the ball. On the other hand, trunnion ball valves have two shafts, top and bottom, which prevent axial displacement of the ball. This reduces wear on the sealing rings and minimizes the influence of fluid pressure on the operational torque, making the operation easier (SOTOODEH, 2021).

In terms of construction, a ball valve can be of the monobloc or split body with 2 or 3 pieces split. A monobloc valve is manufactured as a single piece, without any separate parts, featuring a floating ball. A 2 pieces split body valve is made in two symmetric or asymmetric parts: the body and the cover. In symmetric split body valves, the stem is integral to the ball. In the case of asymmetric split body valves, the stem and ball are separate elements. A 3 pieces split type has a structure consisting of three parts: one body and two covers (SKOUSEN, 2011).

The sizing of ball valves is performed based on standards recognized by manufacturers, clients, and certifying bodies. In this project, we will use the ASME B16.34 standards as a reference. Additionally, we will adopt construction criteria established by the API 6D and ABNT NBR 15827 (2018) standards. With the geometry defined through the design by rules method, we will evaluate the valve using the finite element method, as stipulated by the ASME VIII Division II.

### 2.2 Design by rules - applicable standards

In order to meet the technical requirements of ASME B16.34, the body, flanges, and bolts will be sized according to the nominal diameter and pressure class. Tabulated data from the mentioned standard will be used, and verification will be carried out in accordance with its mandatory appendices. For the flanged connection between the body and the cover, ASME B16.34 provides a strength criterion for the bolts that connect the flanges. The minimum cross-sectional area of the bolt should follow the parameter defined in Equation 1, according to ASME B1.13M for the metric standard.

$$P_c \frac{A_g}{A_b} \leq K_2 S_a \leq 7000, \quad (1)$$

In the equation mentioned, Ag represents the effective gasket area, Pc denotes the pressure class, Sa represents the allowable stress of the bolt at the operating temperature, and K2 is a standardized coefficient with a value of 50.76 /MPa when Sa is expressed in MPa.

According to the API 6D (2014) standard, the sizing of a valve based on the operating pressure should follow the guidelines of ASME VIII Division I or II, ASME B16.34, EN 12516-1, or EN 13445-3. This standard also provides methodologies for sizing bolted connections through flanges and recommends the use of API 6A (2010) for sizing the bolts in terms of preload and torque. By referring to this standard, it is possible to obtain information about the applied

tightening torque, maximum torque, and assess the strength criteria. It is important to note that the applied torque, based on internal pressure or gasket crushing force, should be lower than the strength of the bolts established by API 6A (2010).

According to item 5.1 of ABNT NBR 15827 (2018), a ball valve manufactured in cast or forged steel, with a rating between 150 and 2500, must comply with the construction standard established in Annex C of the same norm, as well as meet the criteria defined by API 6D. Furthermore, the norm also determines that the pressure used for sizing should be the hydrostatic test pressure, which corresponds to 1.5 times the maximum working pressure at ambient temperature.

The designed model considers a split-body trunnion ball valve, NPS 6, pressure class 600, applied in a minimum temperature condition of -29 °C, operating temperature of 38 °C, and maximum temperature of 150 °C. The materials used were ASTM A216 GR WCB for the body and cover, ASTM A193 GR B7 for the bolts, and ASTM A194 GR 2H for the hex nuts. With the geometry obtained through sizing according to normative requirements, the analysis method defined by ASME VIII Division II is applied.

### 2.3 Design by analysis – finite elements method

As a computational tool for elastic, elastoplastic, and localized deformation analysis methods, the commercial software ANSYS Workbench R2018 was used for pre-processing, processing, and post-processing through the static-structural module. The material curve definition, stress linearization, result treatment, and graph plotting were performed using the Python 3 programming language compiled through the Spyder IDE.

In order to reduce computational costs, it was decided to simplify the valve analysis by considering only half of the geometry, taking into account its symmetry. To represent the test condition, flanges were applied at the ends of the valve, in the lever shaft and trunnion cavities, as well as in the trunnion drain plug. To model the physical junction between the components, linear contacts (Bonded and No Separation) were used in the elastic stress analysis, while nonlinear contacts (Bonded and Frictional) were employed in the elastoplastic analysis.

With the geometry and materials defined, the valve was discretized into a finite number of elements and nodes. For this purpose, parabolic elements (TET10) were used in the body, cover, and end flanges, while hexahedral elements (HEX20) were employed in the nuts and bolts due to their regular geometry. In the case of the end flanges, where no specific interest was involved, an automatic mesh was generated, adjusting only the element size, resulting in some elements of type WED15 and PYR13.

The meshing was performed considering the type of element used, as parabolic tetrahedral elements model variable stresses and strains. Thus, each edge of the element corresponds to 1/4 of the smallest valve thickness, providing an appropriate trade-off between result convergence and computational cost. Figure 1a shows the discretized model, Figure 1b illustrates the boundary conditions of the analysis, and Table 1 indicates the mesh quality parameters.

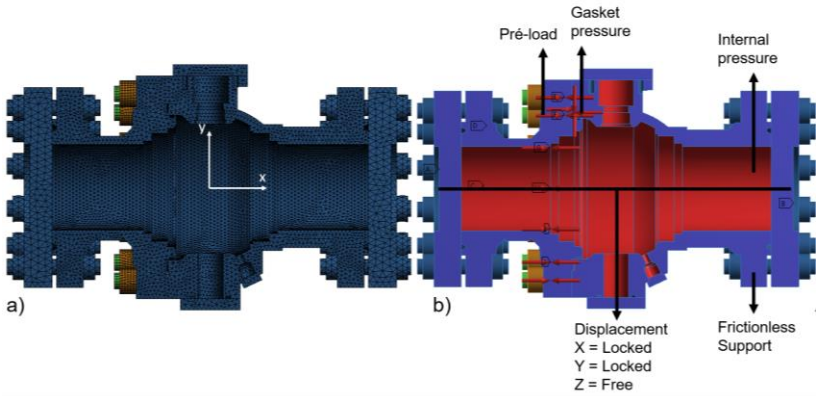


Figure 1 – a) Finite element mesh, b) Boundary conditions

Table 1- Mesh quality parameters

| Parameter | Minimum | Maximum | Average | σ | Target |
|---|---|---|---|---|---|
| Element Quality | 5E-4 | 1.00 | 0.82 | 0.12 | 1.00 |
| Aspect Ratio | 1.00 | 2E5 | 2.70 | 327.00 | 1.00 |
| Warping | 0.00 | 0.33 | 8E-2 | 5E-2 | 0.00 |
| Orthogonal Quality | 3E-8 | 0.99 | 0.76 | 0.15 | 1.00 |
| Jacobian | -1.00 | 1.00 | 0.96 | 0.12 | -1.00 or 1.00 |
| Max. Corner Angle | 62 ° | 179 ° | 97 ° | 13 ° | 90 ° |
| Nodes | | | 559509 | | |
| Elements | | | 342073 | | |

### 2.4 Elastic stress analysis method

For the linear elastic analysis model, constant properties of isotropic materials were used, as shown in Table 2.

Table 2- Isotropic properties of materials used in the project

| Material | Component | Elastic modulus [GPa] | Yield stress [MPa] | Ultimate Stress [MPa] | Poisson's Ratio |
|---|---|---|---|---|---|
| ASTM A-193 GRB7 | Bolts | 200 | 720 | 860 | 0.3 |
| ASTM A-194 GR2H | Nuts | 200 | 720 | 860 | 0.3 |
| ASTM A-216 GRWCB | Body, cover and end flanges | 200 | 250 | 570 | 0.3 |

The material properties were defined based on their respective ASTM standards and input into the software with linear elastic isotropic behavior.

To represent the actual variation of stress along the wall thickness of the valve more accurately, a stress linearization approach was chosen with the applied load paths in the regions of interest in the analysis. This allowed for a more effective assessment of the points of minimum thickness and maximum stress concentration. Figure 2 shows the 22 load paths evaluated for stress linearization, named from L1 to L22.

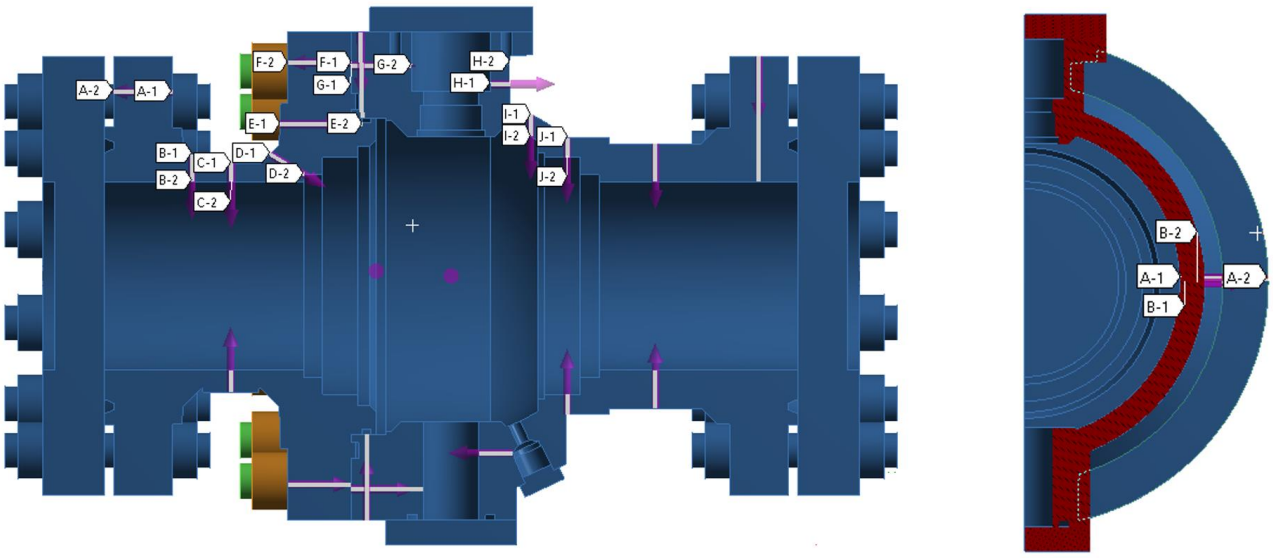


Figure 2 - Load paths for stress linearization

The values of the loads applied in Figure 1b are presented in Table 3. For linear analyses, constant values were used throughout the analysis time.

Table 3 – Magnitude of applied loads

| Load | Value |
|---|---|
| Internal pressure [MPa] | 10.21 |
| Pre-load [kN] | 184.61 |
| Gasket pressure up [MPa] | 27.60 |
| Gasket pressure down [MPa] | 39.40 |
| Gasket pressure right [MPa] | 5.78 |
| Gasket pressure left [MPa] | 5.92 |

The linear analysis was divided into two-time intervals. In the first interval, the pre-load was applied with its nominal value, while in the second interval, the pre-load was kept constant. This condition was adopted to represent the physical behavior of this load, which occurs only at the beginning of the analysis.

According to the guidelines of ASME VIII Division II, it is necessary to consider certain load combinations. In this case, the effects of pressure generated by fluid weight, wind, snow, and moment caused by flow inside the pipeline were

disregarded. This simplification was made because the values of these effects are two orders of magnitude smaller than the internal pressure, making them insignificant in terms of their impact on the results.

After processing the analysis, the values of membrane stress, bending stress, combined membrane and bending stress, peak stress, and total stress were calculated for each defined load path. Subsequently, compliance assessments were conducted according to the criteria established by ASME VIII Division II. The adopted criteria can be found in Table 4, based on the material's yield strength (Sy).

Table 4 – Pass/Fail Criterion for Each Analyzed Failure Mode

| Failure Mode | Pass / fail Criteria | Limit |
|---|---|---|
| Structural collapse | Primary Membrane Stress ≤ S | S = minimum (Sy/1.5; Sut/2.4) |
| | Primary Bending Stress ≤ Spl | Spl = Sy |
| Incremental collapse | Secondary Stress (Membrane + Bending) ≤ Sps | Sps = Sy |
| Fatigue | Peak ≤ Sa | Sa = Curve Attachment 5F ASME VIII Div II |
| Structural collapse | Total Stress ≤ Sy | Sy |

In addition to evaluating the pass/fail criteria, the safety margin was calculated for each load path by comparing the allowable limit to the acting stress.

### 2.5 Elastic-plastic stress analysis

In a linear analysis using the finite element method, throughout the solution of the problem, the stiffness of the structure remains constant, requiring only the assembly of the initial stiffness with the creation of the mesh. However, in many real physical problems, stiffness varies over time, which constitutes nonlinearity. This variation in stiffness can occur due to geometric conditions, material behavior, or specific physical behavior. To solve a nonlinear problem, it is necessary to use a stiffness corrector in the force-displacement relationship, known as the geometric stiffness matrix, which is added to the initial stiffness matrix. Therefore, it can be observed that the method for solving a nonlinear problem is incremental, where the total applied load is divided into sequential increments applied iteratively, seeking a trajectory of equilibrium between internal and external forces, as well as internal and external work (ALVES FILHO, 2012).

The elastic-plastic stress analysis provides a more accurate assessment of the protection against plastic collapse of a component compared to elastic analysis and critical load methods because it more precisely approximates the actual structural behavior by determining a plastic collapse load. This load is obtained by inducing structural instability in the evaluated component.

To model the elastic-plastic behavior of each material, a true stress-strain curve model was used, which includes temperature-dependent hardening behavior as provided in Annex 3-D of the ASME VIII Division II standard and data from ASME II Part D. The stress and strain curves of the materials are presented in Figures 3a and 3b.

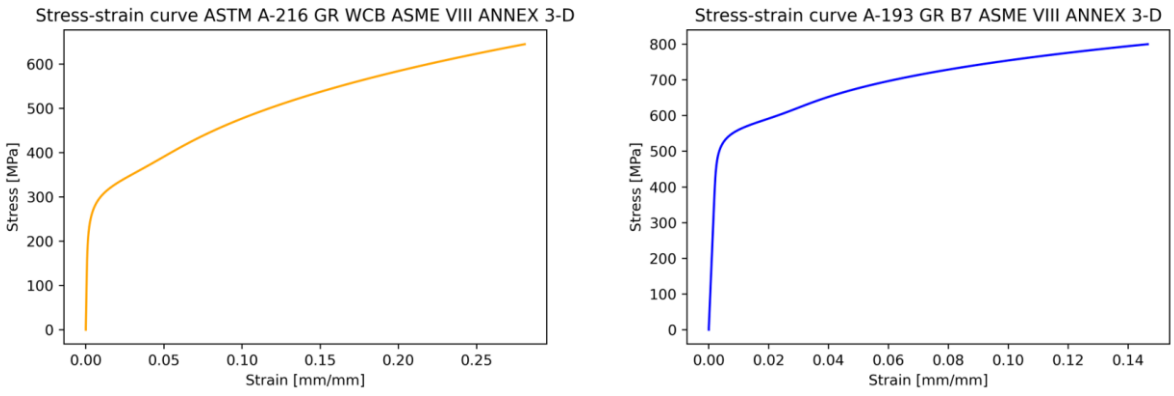


Figure 3 - Stress-strain graphs for the materials used.

When using this material model, the hardening behavior was included up to the true ultimate stress, and perfect plasticity behavior (i.e., the slope of the stress-strain curves is considered zero) beyond this limit. The effects of nonlinear geometry were also considered in this analysis.

To perform the nonlinear analysis, a load combination was applied as shown in Equation 2. This combination was divided into 30 increments, with a minimum of 10 iterations per increment and a maximum of 25 iterations. The resulting stress from joint crushing was kept constant over time, while the pre-load, similar to linear loads, was applied in the first-time interval and kept locked in the subsequent intervals.

$$CMB1 = \beta(P + P_S + D), \tag{2}$$

Where β is a multiplying factor adopted for this analysis as 2.4, as indicated by Table 4.1.3 of ASME VIII Division II, P represents the internal pressure of the line, Ps denotes the static loads of the fluid, and D represents the self-weight of the valve. Only this combination was considered due to the nature of the evaluated component, where wind, snow, and earthquake loads are not significant for the design.

Thus, to perform the analysis, an iterative method was employed using the modified Newton-Raphson procedure. This method was chosen since the Jacobian matrix, which represents the matrix of partial derivatives of the system of equations with respect to the variables of the system, has only its main diagonal inverted and is calculated at each iteration. This reduces the computational cost of the analysis.

For the convergence criterion, a force method was utilized, with a tolerance of 1% set for convergence, and a minimum reference value of 0.01 N. Based on this, the acceptance criteria of the analysis were evaluated according to item 5.2.4.3 of the standard. If analysis convergence is achieved, the component is considered stable under the applied loads for the given case. Otherwise, the component configuration (i.e., thickness) should be modified or the applied loads should be reduced, and the analysis repeated until convergence of the results is obtained.

### 2.6 Elastic-plastic stress analysis - local strain limit

Based on the analysis conducted in the elastic-plastic regime, the principal stresses $\sigma_1, \sigma_2\ e\ \sigma_3$ were obtained, along with the von Mises equivalent stress $\sigma_e$ and the equivalent strain $\varepsilon_{peq}$, for the predefined loading conditions. With these results, it was possible to evaluate localized deformations as described in item 5.3.3 of ASME VIII Division II. To establish a pass/fail strength criterion, the standard defines a limit for localized deformation according to Equation 3.

$$\varepsilon_L = \varepsilon_{Lu} \cdot \exp\left[-\left(\frac{\alpha_{sl}}{1+m_2}\right)\right]\left(\left\{\frac{(\sigma_1+\sigma_2+\sigma_3)}{3\sigma_e}\right\} - \frac{1}{3}\right), \tag{3}$$

The parameters $m_2$, $\alpha_{sl}$ e $\varepsilon_{Lu}$ are defined in Table 5.7 of the standard for different types of materials. As a pass/fail criterion, it is determined that the sum of the equivalent plastic strain and the deformations resulting from the manufacturing process ($\varepsilon_{cf}$) must be less than or equal to the localized limit strain, as shown in Equation 4.

$$\varepsilon_{peq} + \varepsilon_{cf} \leq \varepsilon_L, \tag{4}$$

If this criterion is met, the analyzed component is in compliance with ASME VIII Division II based on the localized strain criterion. As a design consideration, deformations due to the manufacturing process were neglected. Thus, the pass/fail criterion was adopted according to Equation 5.

$$\varepsilon_L - \varepsilon_{peq} \geq 0, \tag{5}$$

In addition to the evaluation based on the difference between the applied and limit strains, the localized strain damage index was also examined. In this procedure, the loading path was divided into 128 load increments, including steps and sub steps. For each load increment, the principal stresses $\sigma_1, \sigma_2\ e\ \sigma_3$, the equivalent stress $\Delta_{ek}$, and the change in equivalent plastic strain relative to the previous load increment $\Delta_{\varepsilon peqk}$ are calculated. The strain limit for the k-th load increment, $\varepsilon_{Lk}$, is determined using Equation 3. The strain damage limit for each load increment is calculated using Equation 6 and evaluated based on the criterion in Equation 7, with deformation effects from forming processes disregarded.

$$De_k = \frac{\Delta\varepsilon_{peqk}}{\varepsilon_{Lk}}, \tag{6}$$

$$\sum_{k=1}^{M} De_k \leq 1, \tag{7}$$

## 3. RESULTS

### 3.1 Design by rules - applicable standards

The data presented in Table 5 were obtained through calculation procedures defined by the ASME B16.34, API 6D, and ABNT NBR 15827 standards. For the design conditions, standardized parameters were adopted, along with technical requirements based on experimental knowledge from manufacturers of these components. Thus, the base geometry took into account the development know-how employed by Micromazza Industria de Válvula LTDA.

Table 5 – Design Parameters Calculated according to the Applicable Standards

| Parameter calculated according to the applicable standards | Value |
|---|---|
| Minimum area required by ASME B16.34 [mm²] | 5858.67 |
| Effective total area subject to bolt tension [mm²] | 7135.47 |
| Minimum total area required in operating condition [mm²] | 5069.12 |
| Actual area of the bolt at the root of the thread [mm²] | 6801.87 |
| Minimum crushing load on the gasket [N] | 392937.9 |
| Design load in gasket crushing condition [N] | 1078418.4 |
| Nominal tightening torque on resistant bolts [Nm] | 1320.0 |
| Maximum tightening torque on resistant bolts [Nm] | 1452.0 |
| Minimum tightening torque on resistant bolts [Nm] | 1188.0 |
| Load due to hydrostatic test pressure [N] | 1046769.1 |
| Design load in operating condition [N] | 986915.6 |
| Minimum crushing load of the gasket [N] | 392937.9 |
| Force required for each fastener [N] | 74769.2 |
| Acting tightening torque on the bolts [Nm] | 534.0 |
| Maximum acting tightening torque on the bolts [Nm] | 588.0 |
| Safety factor for the bolts | 2.46 |
| Margin of safety for the bolts regarding yield strength | 80% |

In this way, it was possible to calculate the pass/fail criteria regarding the strength of the bolts, as shown in Table 6.

Table 6 – Pass/fail criteria for bolts

| Criteria | Condition |
|---|---|
| Effective Total Area Subjected to Bolt Tension ≥ Minimum Required Area (ASME B16.34) | APPROVED |
| Real Area of the Bolt Thread Root ≥ Minimum Total Required Area under Operating Condition (ASME VIII Division II) | APPROVED |
| Torque as per internal pressure ≤ Fastener Strength (API 6A indicated by API 6D) | APPROVED |

### 3.2 Design by analysis – finite elements method

### 3.3 Elastic stress analysis method

The graph in Figure 5 presents the results obtained from the analysis of elastic stresses, summarizing the values of membrane stress, bending stress, membrane + bending stress, peak stress, and total stress, as well as the limits S (Sy/1.5) and Spl and Sps (Sy).

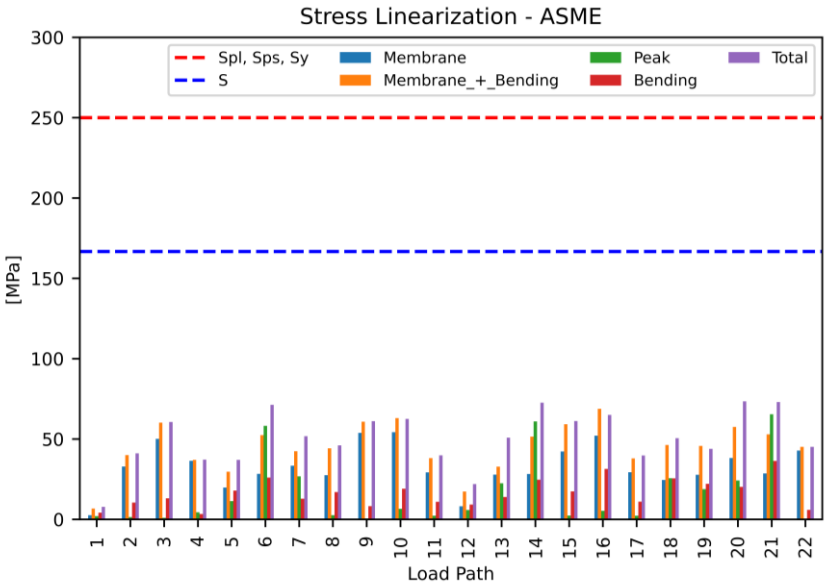


Figure 4 – Stress linearization and limits stress according to ASME VIII Division II

As verified in the previous graph, all linearized stresses evaluated in the valve remain below the limits defined as Sy/1.5 and Sy. Therefore, the analysis was accepted with a pass condition for all load paths. Additionally, the safety margin was assessed, indicating how far each result is from failure. The minimum safety margin obtained was 244%, with an average of 3422% and a standard deviation of 10073%.

### 3.4 Elastic-plastic stress analysis

After defining the analysis conditions in the preprocessing stage, the processing was performed using the ANSYS MAPDL 2022 R2 solver. As a result of the analysis, load step graphs were obtained, showing the number of iterations versus the number of subdivisions of the total load. Additionally, force convergence and force criterion graphs were generated. Both graphs were obtained through data analysis of the software outputs and are presented in Figure 6a and 6b, respectively.

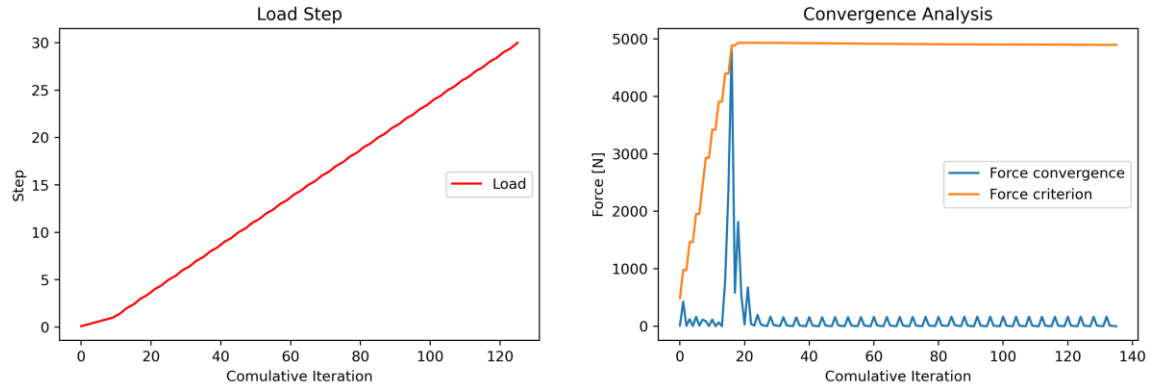


Figure 5 - a) Load Step Graph b) Force Convergence and Force Criterion Graph by Iteration

In Figure 5b, the force convergence measures the difference between the forces calculated in consecutive iterations and checks if this difference is below the pre-established limit. When the difference in forces between consecutive iterations is smaller than this limit, the solution is considered to have converged.

Figure 6 presents the global deformations of the structure, where Figure 7a shows the deformation diagram on the geometry using a color map, while Figure 6b displays the graph of minimum, maximum, and average deformations convergence as a function of iterations.

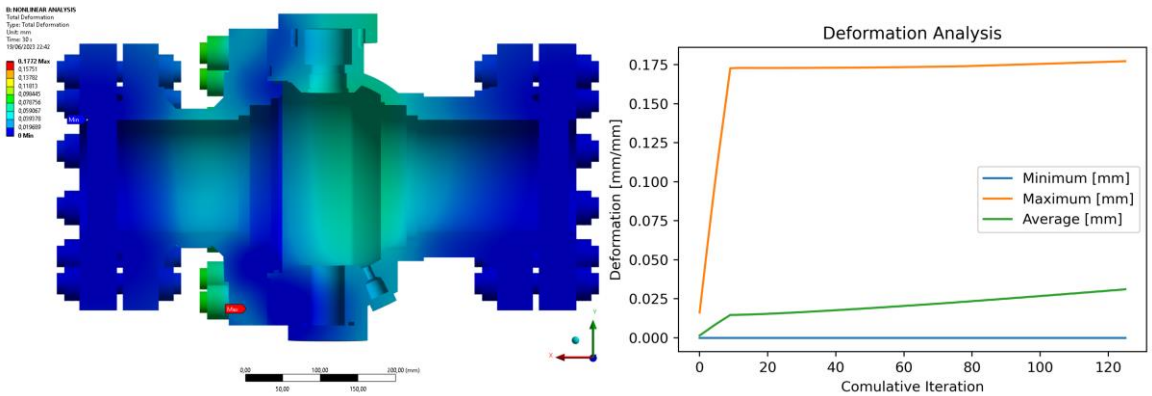


Figure 6 - a) Deformation Diagram b) Deformation Graph per Iterations

By comparing the graphs in Figures 5a, 5b, and 6a, it is possible to observe a convergence of the results, as the 30 load steps were consistently satisfied. The force criterion parameter stabilized, as well as the force convergence, which not only stabilized but also tended towards 0 after a certain stage of the incremental analysis.

Figure 7 shows the distribution of von Mises equivalent stresses for the body, cover, bolts, and nuts that make up the base structure of the valve. This allows for a separate evaluation of stress distribution and facilitates comparisons among different types of materials used. This metric is calculated from the principal stress components obtained using methods such as the Cauchy stress tensor. It represents a material's ability to withstand loads and identifies critical points where failures or excessive deformations may occur. It is important to note that the elastic-plastic analysis assesses the

convergence of results rather than directly comparing them to the material's yield limit, as done in an elastic analysis. This is because the elastic-plastic material model is applied, and the analysis aims to ensure the stability of the structure under the combined loading conditions.

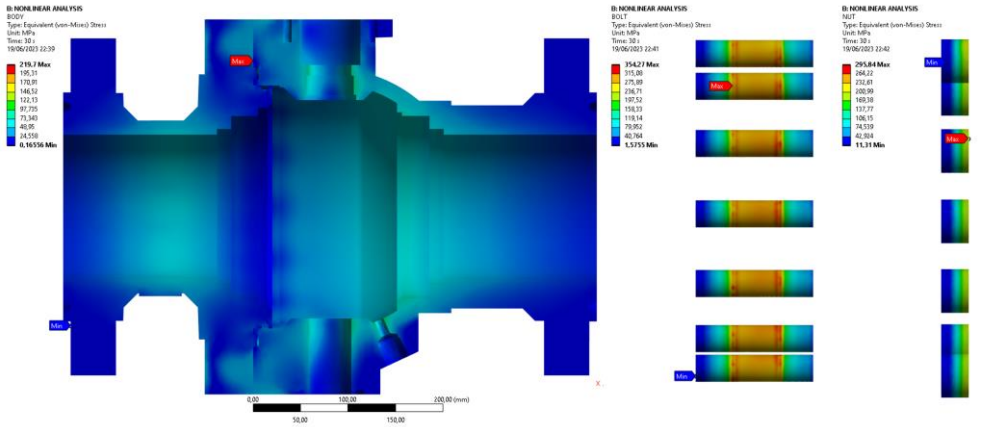

Figure 7 - Equivalent Von Mises Stress for Body, cover, bolts, and nuts

To complement the data presented in Figure 7, the graphs in Figure 8 demonstrate the behavior of von Mises equivalent stresses, minimum stresses, maximum stresses, and average stresses. It is possible to observe a gradual increase in stress until convergence is achieved after a certain number of iterations, and the stress remains stable beyond that point.

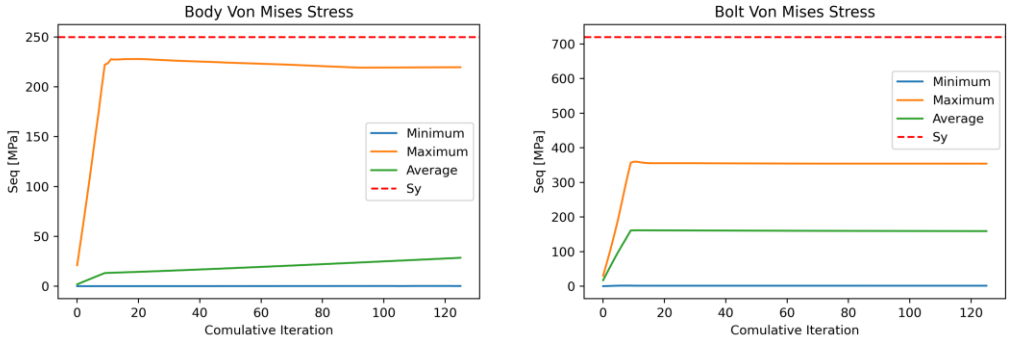


Figure 8 - Equivalent Von Mises Stress: a) Body and cover b) Bolts

### 3.5 Elastic-plastic stress analysis - local strain limit

Figure 9 presents the color map of the distribution of the localized strain criterion in the structure.

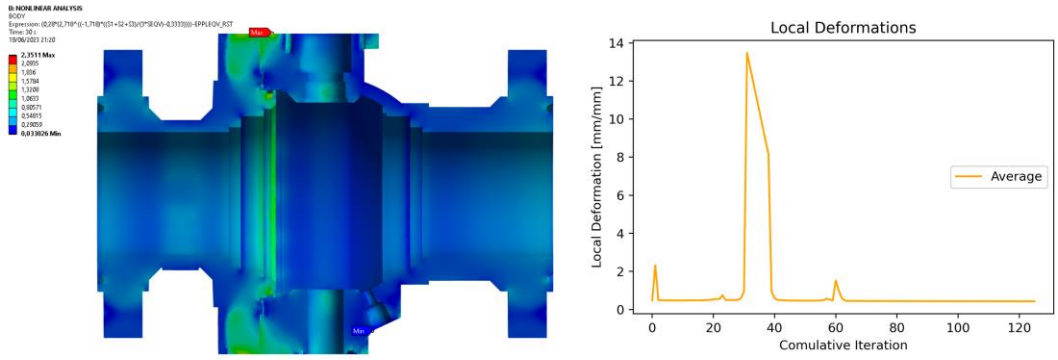


Figure 9 - Distribution of localized deformation criterion using the procedure described by ASME VIII Division II

By evaluating the results obtained from the analysis of localized deformations, it is possible to assess the criteria based on local plastic deformations occurring in critical regions of the structure where the loadings are most intense. Thus, when

evaluating the criterion proposed in Equation 5, it can be observed that all the values are positive, meeting the condition that there will be no localized deformations exceeding the limit proposed by ASME VIII Division II. The strain damage index was also evaluated according to Equation 6, resulting in a value of 0.00064, thus satisfying the criterion of Equation 7.

## 4. CONCLUSION

Based on the sizing according to regulatory requirements, it was possible to obtain an initial geometry for the project using the analysis methodology proposed by ASME VIII Division II. With the geometry, materials, and boundary conditions defined, a finite element model was created to perform two separate analyses.

The first analysis consisted of a linear elastic simplification using the stress linearization method. The safety margins obtained were within the acceptable limits proposed by ASME VIII Division II. Subsequently, an elastoplastic analysis was performed, considering the material behavior according to Annex 3-D of ASME VIII Division II and data from ASME II Part D.

Through this incremental and iterative analysis, it was possible to obtain the actual behavior of the structure, verifying convergence and analyzing deformations and stresses, which remained within the established safety limits. Finally, through an elastoplastic deformation analysis, it was possible to assess the localized behavior of the structure, validating its resistance against this failure mode.

Upon evaluating the obtained results, we can confirm that the project meets the initial objectives, including the requirements of standards such as ASME B16.34, API 6D, and ABNT NBR 15827. Furthermore, the project has been validated through numerical analysis using the design-by-analysis method proposed by ASME VIII Division II. Therefore, the design meets the technical requirements for resistance against plastic collapse and localized failures. However, a fatigue failure analysis under cyclic loading could be considered for future work.

## 5. ACKNOWLEDGEMENTS

The authors would like to express their gratitude to the Federal Technological University of Paraná and Micromazza Industria de Válvula LTDA for their partnership between the academic and business environments, aimed at the development of new technologies in the oil and gas equipment sector.

## 6. REFERENCES

ALVES FILHO, Avelino, 1951- Elementos Finitos: A Base da Tecnologia CAE: Análise não linear / Avelino Alves Filho. – 6. Ed. – São Paulo: Érica, 2012.

AMERICAN PETROLEUM INSTITUTE. API SPECIFICATION 6A: Wellhead and Tree Equipment. 21 ed. Eua: Api, 2019.

AMERICAN PETROLEUM INSTITUTE. API SPECIFICATION 6D: Specification for Valves. 25ed. Eua: Api, 2021.

ASSOCIAÇÃO BRASILEIRA DE NORMAS TÉCNICAS. NBR 15827: Válvulas industriais para instalações de exploração, produção, refino e transporte de produtos de petróleo - Requisitos de projeto e ensaio de protótipo. 6 ed. São Paulo: Abnt, 2022.

ECOM. Setor de óleo e gás. 2020. Disponível em: bit.ly/3gHl8MB. Acesso em: 25 out. 2022.

JEFFERSON. Válvulas de Esfera. 2020. Disponível em: bit.ly/3N4w0QO. Acesso em: 25 out. 2022.

MORAES, Osvaldo. Válvulas Industriais. Rio de Janeiro: Petrobras, 2005.

ROSSETTO, Diego Rizzotto. Avaliação da integridade estrutural de projetos de válvulas do tipo esfera trunnion e/ou gaveta utilizadas nas instalações de petróleo. 2016. 177 f. Tese (Doutorado) - Curso de Engenharia de Minas,

SKOUSEN, Philip L. Valve Handbook. 3. ed. Utah: McGraw-Hill Professional Publishing, 2011.

SOTOODEH, Karan. A practical guide to piping and valves for the oil and gas industry. Oslo: Gulf Professional Publishing, 2021. 968 p.

THE AMERICAN SOCIETY OF MECHANICAL ENGINEERS. ASME B16.34: Valves- -Flanged, Threaded, and Welding End. Eua: Asme, 2020. 228 p.

THE AMERICAN SOCIETY OF MECHANICAL ENGINEERS. ASME BPVC-II: BPVC Section II-Materials-Part D-Properties-(Customary). Eua: Asme, 2023. 1260 p.

THE AMERICAN SOCIETY OF MECHANICAL ENGINEERS. ASME BPVC-VIII-2: BPVC Section VIII-Rules for Construction of Pressure Vessels Division 2-Alternative Rules. Eua: Asme, 2019. 872 p.

## 7. RESPONSIBILITY NOTICE

The authors are the only responsible for the printed material included in this paper.